Electric circuits for universal quantum gates and quantum Fourier transformation

Motohiko Ezawa
Department of Applied Physics, University of Tokyo, Hongo 7-3-1, 113-8656, Japan

Universal quantum computation may be realized based on quantum walk, by formulating it as a scattering problem on a graph. In this paper, we simulate quantum gates through electric circuits, following a recent report that a one-dimensional LC electric circuit can simulate a Schrödinger equation and hence a quantum walk. Especially, we propose a physical realization of a set of universal quantum gates consisting of the CNOT, Hadamard and $\pi/4$ phase-shift gates with the use of telegrapher wires and mixing bridges. Furthermore, we construct the $\pi/2^n$ phase-shift gate for an arbitrary integer n, which is an essential element to perform the quantum Fourier transformation and prime factorization based on the Shor algorithm. Our results will open a way to universal quantum computation based on electric circuits.

arXiv:1911.02250v2 [cond-mat.mes-hall] 4 Dec 2019

Quantum computation[1,2] is a most urgent and promising next generation technique, which overcomes the limit of the Moore law. Universal quantum computation is indispensable to make any quantum algorithms possible[3]. According to the Solovay-Kitaev theorem, a set of the universal gates consists of two Clifford and one non-Clifford gates[4]. The standard set is given by the controlled-NOT (CNOT), Hadamard and $\pi/4$ phase-shift gates[5], where the $\pi/4$ phase-shift gate is a non-Clifford gate. Any unitary transformation is executable with the use of these operators. One of the method to realize universal quantum computation is based on quantum walks[6–11], where widgets act as quantum gates. However, it is still a long-standing problem how to achieve a physical realization of these gates on the basis of quantum walks.

Recently, electric circuits attract much attention in the context of topological physics[12–23]. Majorana-like topological edge states can be simulated in electric circuits[22], and scalable topological quantum computation would be possible based on their braiding[24]. On the other hand, it is shown[25] that quantum walks are simulated by the telegrapher circuit because the mathematical equivalence holds between the telegrapher equation and the Schrödinger equation.

In this paper, we present a physical realization of a set of the CNOT, Hadamard and $\pi/4$ phase-shift gates with the use of LC electric circuits. We consider a telegrapher circuit, which we map to a graph G by identifying nodes and links as vertices and edges, respectively. We introduce a subdivided graph G' by transforming a link to a vertex. The graph G' is bipartite since it involves two types of vertices, representing voltage and current physically. The simplest example is the one-dimensional telegrapher wire illustrated in Fig.1(a), which corresponds to graphs G and G' in Fig.1(b) and (c), respectively. Quantum walks on graph G' have already been explored[25]. We note that, once a subdivided graph is given, the corresponding electric circuit is readily designed.

The next-simplest telegrapher circuit consists of four semi-infinite wires for two inputs and two outputs, connected to a certain finite circuit called a widget. It corresponds to a quantum gate represented by a 2×2 matrix. There are three building blocks, the mixing gate $U_{\rm mix}^{(2)}$, the ϕ phase-shift gate U_ϕ and the Pauli X gate $U_X\equiv\sigma_x$, where

$$U_{\rm mix}^{(2)}\equiv\frac{1}{\sqrt{2}}\begin{pmatrix} i & -1\\ -1 & i\end{pmatrix},\qquad U_\phi=\begin{pmatrix}1 & 0\\ 0 & e^{i\phi}\end{pmatrix}. \tag{1}$$

The mixing gate corresponds to the one named "basis-changing gate" in literature[6]. The phase-shift gate U_ϕ is constructed simply by inserting inductors due to the induced electromotive force. However, the mixing gate contains two bridges across two wires as in Fig.2, and causes a back scattering of quantum walkers by the bridges. Note that the superscript (2) in $U_{\rm mix}^{(2)}$ implies the number of the bridges. The suppression of back scattering is necessary for quantum computing, which restricts the momentum associated with a quantum walker. Possible values of the phase shift ϕ are determined by this condition. The phase shift $\phi=\pi/4$ is such an allowed one, producing the $\pi/4$ phase-shift gate as in Fig.3. The Hadamard gate is constructed as in Fig.4(a) in accord with the relation $U_{\rm H}=-iU_{3\pi/2}U_{\rm mix}^{(2)}U_{3\pi/2}$, where $U_{3\pi/2}=(U_{\pi/4})^3$. The X gate is simply given by exchanging two wires as in Fig.4(b). The CNOT gate transforms four inputs to four outputs, whose main part is the X gate as in Fig.4(d). The standard set of univesal gates is constructed in this way.

A most important application of quantum computers is prime factorization. A key algorithm is the quantum Fourier transformation. It is decomposed into the Hadamard gate $U_{\rm H}$ and the $\pi/2^n$ phase-shift gate with integer n in (1). Although any quantum gate may be constructed based on the standard set of universal gates, it is better to employ the $\pi/2^n$ phase-shift gate directly for practical purpose. We are able to construct it together with the mixing gate $U_{\rm mix}^{(N)}$ by introducing N bridges across two wires with $N=2^{n-1}$ as in Fig.5.

Here we summarize the main differences between the previous studies[6–8] and the present one as graph theory. First, the graph is bipartite because it describes a network of voltage and current in the electric-circuit realization. Second, the hopping parameters are pure imaginary as in (5), as originates in the mapping of the telegrapher equation to the Schrödinger equation. Third, the amplitude of the hopping is not uniform because we use two types of inductors L and L' as in Fig.2, which makes the graph weighted.

Quantum walks and telegrapher equation: Our basic idea is to use telegrapher wires for a physical realization of quantum walks. A telegrapher wire is a playground of one-dimensional quantum walkers[25], where each node is connected to the ground by capacitor C, and to each link an inductor L is inserted, as illustrated in Fig.1. We also consider a widget connected to semi-infinite wires. For example, there are two input wires and two output wires connected to a widget marked in

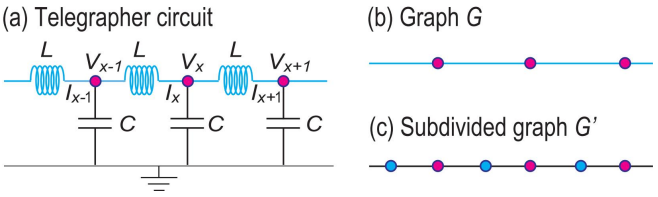


FIG. 1: (a) Illustration of a one-dimensional telegrapher circuit, where two nodes (in magenta) are connected by inductor L in cyan. Each node is connected to the ground by capacitor C. (b) Illustration of the associated graph G. (c) Illustration of the subdivided graph G', where cyan vertices correspond to inductors L.

green in Fig.2. The key problem is whether a quantum walker may get through it without reflection.

An LC electric circuit is characterized by the Kirchhoff laws for the voltage V_x at the node x and the current I_x entering to the node x,

$$L_x \frac{d}{dt} I_x(t) = V_{x'}(t) - V_x(t), \tag{2}$$

$$C_x \frac{d}{dt} V_x(t) = I_x(t) + \sum_{x'} (-1)^s I_{x'}(t), \tag{3}$$

where x' is one of the neighboring nodes of x such that the current is I_x between these two nodes. The sign s is determined whether the current is in-going or out-going. The first equation is the Kirchhoff voltage law with respect to the voltage difference between two nodes V_x and $V_{x'}$, which originates in the induced electromotive force by the inductor L_x. The second equation is the Kirchhoff current law with respect to the current conservation at one node V_x. We denote a vertex representing the voltage V_x (the current I_x) in magenta (cyan) in figures.

We may rewrite the Kirchhoff laws (2) and (3) in the form of the Schrödinger equation on the graph G,

$$i \frac{d}{dt} \psi(x,t) = H\psi(x,t), \tag{4}$$

as we have presented a concrete example for one-dimensional quantum walks elsewhere[25]. Here, the wave function is a two-component vector, $\psi(x,t) = (\mathcal{I}_x(t), \mathcal{V}_x(t))^t$, with $\mathcal{V}_x(t) = V_x(t)$ and $\mathcal{I}_x(t) = \sqrt{L/C} I_x(t)$. The Hamiltonian H is given by the Kirchhoff laws when an electric circuit is given.

We make separation of variables, $V_x(t) = \mathrm{Re}[V(x) e^{i\omega t}]$ and $I_x(t) = \mathrm{Re}[I(x) e^{i\omega t}]$, where $V(x)$ and $I(x)$ are complex voltage and current. Correspondingly, we define the complex function $\psi(x)$ by $\psi(x,t) = \mathrm{Re}[\psi(x) e^{i\omega t}]$.

The aim of this paper is to propose a set of widgets which act as a set of universal gates. The first step is to solve the Hamiltonian problem of an infinite one-dimensional wire, where the Hamiltonian is given by[25]

$$H = \frac{2}{\sqrt{LC}} \sum_x \left(i |\psi(x)\rangle \langle \psi(x+1)| - i |\psi(x+1)\rangle \langle \psi(x)| \right). \tag{5}$$

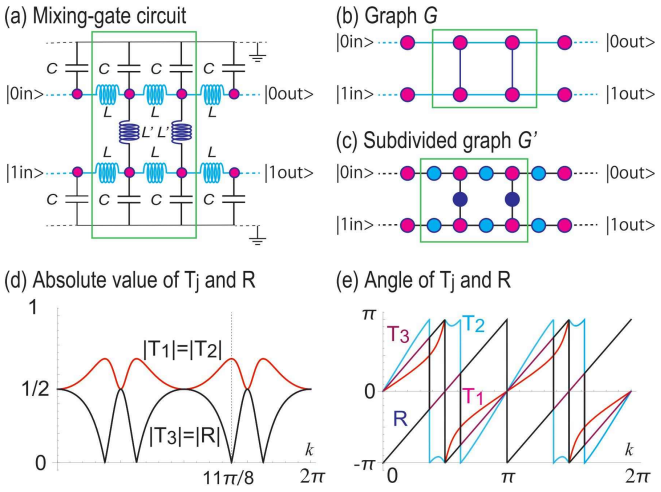


FIG. 2: (a) Illustration of an electric circuit realizing the mixing gate $U^{(2)}_{\mathrm{mix}}$ marked by a green rectangle. It consists of two parallel wires bridged by two inductors L'. (b) Graph G for the mixing gate. (c) The dynamics of the electric circuit is equivalent to a quantum walk on the subdivided graph G'. (d)–(e) The k dependence of the absolute value and the phase of the transmission coefficients $T_1(k)$, $T_2(k)$, $T_3(k)$ and the reflection coefficient $R(k)$. T_1 is colored in red, T_2 is colored in cyan, T_3 is colored in violet and R is colored in black. The horizontal axis is the momentum $0 \le k \le 2\pi$. We find $|T_1(k)| = |T_2(k)|$ and $|T_3(k)| = |R(k)|$.

This Hamiltonian is diagonalized after Fourier transformation, $H = \sum_k E(k) |\psi_k\rangle \langle \psi_k|$, where the eigen-energy is obtained as $E(k) = (2/\sqrt{LC}) \sin k$.

Then, we solve the Schrödinger equation (4) for a system where semi-infinite wires are connected to a widget[6]. The key point is to formulate the system as a scattering problem on a graph, where the wave function is given by solving the eigen-equation[6–8]

$$H\psi_k(x) = (2/\sqrt{LC}) \sin k \psi_k(x), \tag{6}$$

by requiring that the eigen-energy is the same as that of the semi-infinite wire.

Scattering theory on graphs: We start with a one-qubit gate U from the input $(|0\rangle_{\mathrm{in}}, |1\rangle_{\mathrm{in}})$ to the output $(|0\rangle_{\mathrm{out}}, |1\rangle_{\mathrm{out}})$. We realize it by a set of two telegrapher wires containing a finite number of widgets, $U = U_1 U_2 \cdots$. We first analyze a widget illustrated in Fig.2(a) explicitly, where two telegrapher wires are bridged by two inductors L'.

Linear electric circuits satisfy the superposition principle. Hence, it is enough to calculate the transmission and reflection coefficients when we input a plane wave only to the wire $|0\rangle_{\mathrm{in}}$. There are three other lines, where two of them are the outputs and the rest is the other input. This is a scattering problem, and the wave functions are written in the form of

$$\langle x,0|\psi\rangle = e^{-ikx} + R(k) e^{i(k+\pi)x}, \tag{7}$$

$$\langle x,j|\psi\rangle = T_j(k) e^{ikx}, \tag{8}$$

where T_1 and T_2 are for the two outputs, while T_3 is for the other input $j = 1,2,3$. The momentum of the reflected wave

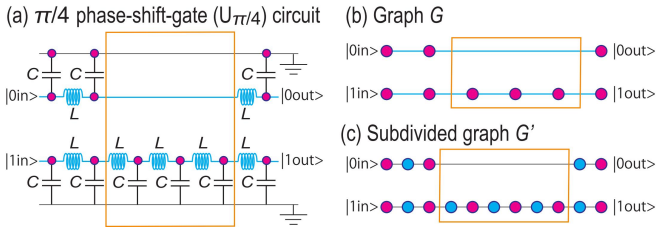


FIG. 3: (a) Illustration of an electric circuit for the $\pi/4$ phase-shift gate. Within the widget, there are no electronic parts in the upper wire, while there are three inductors L in the lower wire, producing the phase delay $2mk_0$ with $m = 3$ in the lower wire compared to the upper wire. (b)–(c) Associated graphs.

is $k+\pi$ in order to preserve the energy $E(k)$. In order to make a quantum gate, it is necessary to determine the momentum $k = k_0$ by requiring $R(k_0) = 0$ and $T_3(k_0) = 0$ since the current should not backflow to the two inputs.

By solving the eigen-equation (6), we obtain

$$T_1(k) = \frac{e^{-2ik} + 2\ell + e^{2ik}\left(2\ell^2 - 1\right)}{e^{-4ik} + e^{-2ik}4\ell + (4\ell^2 - 1)}, \tag{9}$$

$$T_2(k) = \frac{2\ell\left(e^{2ik}\ell + 1\right)}{e^{-4ik} + 4e^{-2ik}\ell + (4\ell^2 - 1)}, \tag{10}$$

$$T_3(k) = \frac{2\ell\left(\ell + \cos 2k\right)}{e^{-4ik} + 4e^{-2ik}\ell + (4\ell^2 - 1)}, \tag{11}$$

$$R(k) = \frac{-2\ell\left(\ell + \cos 2k\right)}{e^{-4ik} + 4e^{-2ik}\ell + (4\ell^2 - 1)}, \tag{12}$$

where $\ell = L'/L$. The reflection becomes zero, $R(k_0) = 0$, at $k_0 \equiv \pm\frac{1}{2}\arccos(-\ell) + \eta\pi$ with $\eta = 0, 1$. At this momentum k_0, it follows that $T_3(k_0) = 0$, $T_1(k_0) = \pm i\sqrt{1-\ell^2}$ and $T_2(k_0) = -\ell$. Hence we obtain

$$U_{\rm mix}^{(2)\pm} = \begin{pmatrix} \pm i\sqrt{1-\ell^2} & -\ell \\ -\ell & \pm i\sqrt{1-\ell^2} \end{pmatrix} \tag{13}$$

for a possible widget acting as a quantum gate.

The Hadamard gate $U_{\rm H}$ is given by

$$U_{\rm H} \equiv \frac{1}{\sqrt{2}}\begin{pmatrix} 1 & 1 \\ 1 & -1 \end{pmatrix}. \tag{14}$$

In order to construct it from $U_{\rm mix}^{(2)\pm}$, we need to set $|T_1(k)| = |T_2(k)|$, which is achieved by choosing $\ell = 1/\sqrt{2}$. Then, $U_{\rm mix}^{(2)+}$ is realized at momenta $k_0 = 3\pi/8, 11\pi/8$, while $U_{\rm mix}^{(2)-}$ is realized at momenta $k_0 = 5\pi/8, 13\pi/8$.

We show the transmission and reflection coefficients as a function of k for $\ell = 1/\sqrt{2}$ in Fig.2(d) and (e). We find $|T_1(k)| = |T_2(k)|$ and $|R(k)| = |T_3(k)|$ for all k.

Phase-shift gate: We construct a phase-shift gate. It is simply constructed by inserting m inductors only in the lower wire compared to the upper wire as shown in Fig.3. The transmission and reflection coefficients are given by $T(k) = e^{2imk}$ and $R(k) = 0$. The transmission is perfect irrespective of the momentum since $|T(k)| = 1$. Consequently, we obtain the ϕ

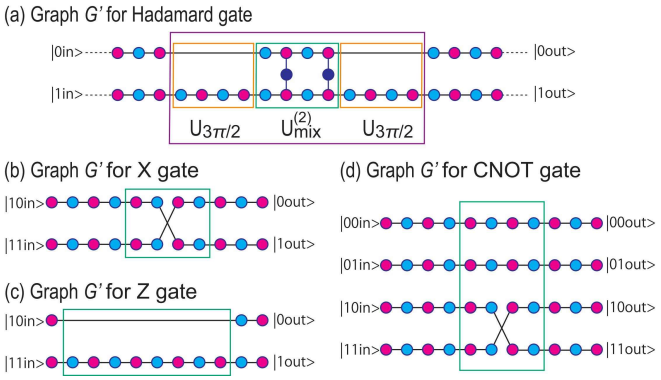


FIG. 4: (a) Graph representation of the Hadamard gate, which consists of the successive operations of the $3\pi/2$ phase-shift and mixing gates. (b)–(d) Graph representation of the Pauli X gate, the Pauli Z gate and the CNOT gate.

mixing-gate U_ϕ with $\phi = 2mk$. It is understood physically that inserted inductors cause delay in the lower wire.

Here the momentum for a phase-shift gate should be the same as that for the mixing gate in one circuit. Then, we need to choose one momentum from $k_0 = 3\pi/8, 11\pi/8, 5\pi/8, 13\pi/8$ for one circuit. Hereafter we choose $k_0 = 11\pi/8$ since it requires the minimum number of inductors to construct the $\pi/4$ phase-shift gate.

By using three inductors, i.e., $m = 3$ and $k_0 = 11\pi/8$, we obtain the $\pi/4$ phase-shift gate as in (1). In general, by inserting m inductors in one wire, we may generate the phase shift $\phi = 2mk_0$. Two successive operations of the $\pi/4$ phase-shift gate yield $U_{\pi/2} = U_{\pi/4}^2$ =diag.$(1, i)$, which is simply called the phase gate.

Hadmard gate: The Hadamard gate is the unitary operation $U_{\rm H}$ defined by (14). It is given by the combination of the mixing and $3\pi/2$ phase-shift gates as $U_{\rm H} = -iU_{3\pi/2}U_{\rm mix}U_{3\pi/2}$, where the $3\pi/2$ phase-shift gate is constructed by inserting two inductors sequentially. We show the graph G' for the Hadamard gate in Fig.4.

Pauli gates: We study the NOT gate. It is defined by the interchange of two inputs $|0\rangle_{\rm in}$ and $|1\rangle_{\rm in}$, or $|1\rangle_{\rm out} = U_X|0\rangle_{\rm in}$ and $|0\rangle_{\rm out} = U_X|1\rangle_{\rm in}$. Such a gate is obviously given by the Pauli X gate, $U_X = \sigma_x$. In terms of electric circuits, two telegrapher wires are simply interchanged as shown in Fig.4(b).

The Pauli Z gate reads $U_Z = \sigma_z$. It is constructed by inserting four successive inductors only for the lower wire as shown in Fig.4(c), because $2mk_0 = \pi$ mod(2π) with $m = 4$. The Pauli Y gate reads $U_Y = iU_XU_Z = \sigma_y$, which is constructed by the successive operations of the Pauli Z and X gates.

CNOT gate: The CNOT gate is a two-qubit gate U, transforming the input $(|00\rangle_{\rm in}, |01\rangle_{\rm in}, |10\rangle_{\rm in}, |11\rangle_{\rm in})$ to the output $(|00\rangle_{\rm out}, |01\rangle_{\rm out}, |10\rangle_{\rm out}, |11\rangle_{\rm out})$. It is defined by

$$U_{\rm CNOT} \equiv \begin{pmatrix} I_2 & O_2 \\ O_2 & U_X \end{pmatrix}, \tag{15}$$

where I_2 is the two dimensional identity matrix and O_2 is the two dimensional null matrix. Its construction is straightforward. We show the graph for the CNOT gate in Fig.4(d).

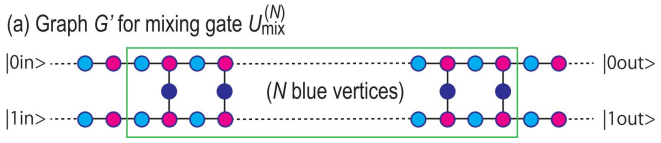


FIG. 5: (a) Graph G' representation of the mixing gate $U_{\rm mix}^{(N)}$ with $N = 2^{n-1}$, which is composed of two wires bridged by N inductors L' (in blue). It is used to construct the $\pi/2^n$ phase-shift gate.

$\pi/2^n$ phase-shift gate: We now construct the $\pi/2^n$ phase-shift gate for arbitrary integer n. First, we construct a mixing gate which matches with the $\pi/2^n$ phase-shift gate, by generalizing the result for the $\pi/4$ phase-shift gate. We bridge two telegrapher wires by $N = 2^{n-1}$ inductors with inductance L', as illustrated in Fig.5. The momentum k_0 and the inductance $L' = \ell L$ should be determined so that there are no reflections to the inputs. The condition is satisfied when we choose $k_0 = 5\pi/4 + \pi/(4N)$ and $\ell = -\cos 2k_0$, where the system acts as the quantum gate given by

$$U_{\rm mix}^{(N)} = \frac{e^{i\pi N/2}}{\sqrt{2}} \begin{pmatrix} \exp\left[-\frac{i\pi}{2}\left(\frac{1}{2}+\frac{1}{N}\right)\right] & \exp\left[\frac{i\pi}{2}\left(\frac{1}{2}-\frac{1}{N}\right)\right] \\ \exp\left[\frac{i\pi}{2}\left(\frac{1}{2}-\frac{1}{N}\right)\right] & \exp\left[-\frac{i\pi}{2}\left(\frac{1}{2}+\frac{1}{N}\right)\right] \end{pmatrix}, \tag{16}$$

for $N \geq 4$. It is reduced to $U_{\rm mix}^{(2)}$ in (1) for $n = 2$ or $N = 2$, where $k_0 = 11\pi/8$ and $\ell = -\cos 11\pi/4 = 1/\sqrt{2}$.

The $\pi/2^n$ phase-shift gate is constructed by inserting m inductors only in the lower wire as for the case of the $\pi/4$ phase shift gate, yielding U_ϕ in (1) with $\phi = 2mk_0$, where m is determined by the condition $2mk_0 = \pi/2^n \ \mathrm{mod}(2\pi)$.

The Hadamard gate is constructed so as to realize the mathematical relation

$$\exp\left[\frac{i\pi}{2}\left(\frac{1}{2}+\frac{1}{N}+N\right)\right] U_{3\pi/2} U_{\rm mix}^{(N)} U_{3\pi/2} = U_{\rm H}, \tag{17}$$

where the $3\pi/2$ phase-shift gate $U_{3\pi/2}$ is constructed from the $\pi/2^n$ phase-shift gate as $U_{3\pi/2} = (U_{\pi/2^n})^{3N}$.

In general we may construct the ϕ phase-shift gate U_ϕ for arbitrary ϕ from the $\pi/2^n$ phase-shift gate as $U_\phi = (U_{\pi/2^n})^s$ with a certain integer s. It is well known that the relation $s/N = 2\phi/\pi$ holds within a required accuracy by taking two integers s and N appropriately.

Quantum Fourier transformation: The quantum Fourier transformation is defined by[26]

$$|k\rangle = \frac{1}{\sqrt{N}} \sum_{j=0}^{N-1} \omega_N^{jk} |j\rangle \tag{18}$$

with $\omega_N = e^{2\pi i/N}$. It is constructed by successive operations of the Hadamard and $2\pi/N$ phase-shift gates[27]. Thus, we are able to perform quantum Fourier transformation with arbitrary large N. See some examples in Supplementary Material[28].

Furthermore, it is possible to construct other multi-qubit gates such as the CZ (controlled-Z), SWAP, Toffoli (controlled-controlled-NOT) and Fredkin (controlled-SWAP) gates[28]. Various arithmetic operations can be made by combinations of the NOT, CNOT and Toffoli gates[29].

We have proposed a physical realization of quantum gates based on quantum walks with the use of electric circuits. When we use inductors of the order of 1nH and capacitors of the order of 1pF, the resonant frequency exceeds 1GHz. Then, we expect high speed quantum computations. Our results will open a way to universal quantum computers made of relatively simple electric circuits. Great merits are that we may control them by classical computers seamlessly integrated and that they work at room temperature.

The author is very much grateful to E. Saito and N. Nagaosa for helpful discussions on the subject. This work is supported by the Grants-in-Aid for Scientific Research from MEXT KAKENHI (Grants No. JP17K05490, No. JP15H05854 and No. JP18H03676). This work is also supported by CREST, JST (JPMJCR16F1).

[1] R. Feynman, Int. J. Theor. Phys. 21, 467 (1982).
[2] D. P. DiVincenzo, Science 270, 255 (1995).
[3] D. Deutsch, Proceedings of the Royal Society A. 400, 97 (1985)
[4] C. M. Dawson and M. A. Nielsen arXiv:quant-ph/0505030.
[5] M. Nielsen and I. Chuang, Quantum Computation and Quantum Information, Cambridge University Press, 2016, p. 189; ISBN 978-1-107-00217-3.
[6] A. M. Childs, Phys. Rev. Lett. 102, 180501 (2009).
[7] M. Varbanov and T. A. Brun, Phys. Rev. A 80, 052330 (2009).
[8] Benjamin A. Blumer, M. S. Underwood, and D. L. Feder, Phys. Rev. A 84, 062302 (2011).
[9] A. P. Hines and P. C. E. Stamp, Phys. Rev. A 75, 062321 (2007).
[10] N. B. Lovett, S. Cooper, M. Everitt, M. Trevers, V. Kendon, Phys. Rev. A. 81, 042330 (2010).
[11] A. M. Childs, D. Gosset, Z. Webb, Science 339, 791 (2013).
[12] C. H. Lee , S. Imhof, C. Berger, F. Bayer, J. Brehm, L. W. Molenkamp, T. Kiessling and R. Thomale, Communications Physics, 1, 39 (2018).
[13] S. Imhof, C. Berger, F. Bayer, J. Brehm, L. Molenkamp, T. Kiessling, F. Schindler, C. H. Lee, M. Greiter, T. Neupert, R. Thomale, Nat. Phys. 14, 925 (2018).
[14] M. S.-Garcia, R. Susstrunk and S. D. Huber, Phys. Rev. B 99, 020304 (2019).
[15] T. Helbig, T. Hofmann, C. H. Lee, R. Thomale, S. Imhof, L. W. Molenkamp and T. Kiessling, Phys. Rev. B 99, 161114 (2019).
[16] E. I. Rosenthal, N. K. Ehrlich, M. S. Rudner, A. P. Higginbotham, and K. W. Lehnert, Phys. Rev. B 97, 220301(R) (2018).
[17] Y. Lu, N. Jia, L. Su, C. Owens, G. Juzeliunas, D. I. Schuster and J. Simon, Phys. Rev. B 99, 020302 (2019).
[18] M. Ezawa, Phys. Rev. B 98, 201402(R) (2018).
[19] T. Hofmann, T. Helbig, C. H. Lee, M. Greiter, R. Thomale, Phys. Rev. Lett. 122, 247702 (2019).
[20] K. Luo, R. Yu and H. Weng, Research (2018), ID 6793752.
[21] M. Ezawa, Phys. Rev. B 99, 201411(R) (2019).
[22] M. Ezawa, Phys. Rev. B 100, 045407 (2019).
[23] T. Helbig, T. Hofmann, S. Imhof, M. Abdelghany, T. Kiessling, L. W. Molenkamp, C. H. Lee, A. Szameit, M. Greiter, R. Thomale, arXiv:1907.11562.

[24] M. Ezawa, cond-mat/arXiv:1907.06911.
[25] M. Ezawa, Phys. Rev. B 100, 165419 (2019).
[26] D. Coppersmith, Technical Report RC19642, IBM (1994)
[27] M. Nielsen and I. Chuang, Quantum Computation and Quantum Information. Cambridge: Cambridge University Pres (2000).
[28] See Supplemental Material II for results on the CZ, SWAP, Toffoli and Fredkin gates.
[29] V. Vedral, A. Barenco and A. Ekert, Phys. Rev. A 54, 147 (1996)

Supplemental Material

In the main text, we have constructed a set of the CNOT, Hadamard and $\pi/4$ phase-shift gates with the use of LC circuits. Here we present graphs G' for some other typical gates, from which the corresponding LC circuits are readily written down.

Square root of the NOT gate: The square roof of the NOT gate U_X is given by

$$U_{\sqrt{X}} \equiv \frac{1}{2}\begin{pmatrix} 1+i & 1-i \\ 1-i & 1+i \end{pmatrix}, \tag{S1}$$

so that $U_{\sqrt{X}}^2 = U_X$. It is realized by the sequential application of the NOT gate and the mixing gates as

$$U_{\sqrt{X}} = -e^{i\pi/4} U_{\text{mix}}^{(2)} U_X. \tag{S2}$$

One-qubit universal gate: The one-qubit universal quantum gate is constructed in the combination of the Hadamard and the phase-shift gates as

$$U_{\text{1bit}} = e^{-i\theta/2} U_{\phi+\pi} U_{\text{H}} U_\theta U_{\text{H}} = \begin{pmatrix} \cos\frac{\theta}{2} & -i\sin\frac{\theta}{2} \\ ie^{i\phi}\sin\frac{\theta}{2} & -e^{i\phi}\cos\frac{\theta}{2} \end{pmatrix}. \tag{S3}$$

SWAP gate: The SWAP gate is defined by

$$U_{\text{SWAP}} \equiv \begin{pmatrix} 1 & 0 & 0 & 0 \\ 0 & 0 & 1 & 0 \\ 0 & 1 & 0 & 0 \\ 0 & 0 & 0 & 1 \end{pmatrix}. \tag{S4}$$

It is constructed by the exchange of the wires between $|01\rangle_{\text{in}}$ and $|10\rangle_{\text{in}}$, which are shown in Fig.S1. The SWAP gate exchanges two qubits as

$$U_{\text{SWAP}} |j_2 j_1\rangle = |j_1 j_2\rangle. \tag{S5}$$

CZ gate: The controlled-Z (CZ) gate is defined by

$$U_{\text{CZ}} \equiv \begin{pmatrix} I_2 & O_2 \\ O_2 & U_{\text{Z}} \end{pmatrix} = \begin{pmatrix} 1 & 0 & 0 & 0 \\ 0 & 1 & 0 & 0 \\ 0 & 0 & 1 & 0 \\ 0 & 0 & 0 & -1 \end{pmatrix}. \tag{S6}$$

We realize it by inserting four inductors only for the wire representing $|11\rangle_{\text{out}}$.

Controlled phase-shift gate: The controlled phase shift gate $U_{2\to\phi}$ is defined by

$$U_{2\to\phi} \equiv \begin{pmatrix} I_2 & O_2 \\ O_2 & U_\phi \end{pmatrix} = \begin{pmatrix} 1 & 0 & 0 & 0 \\ 0 & 1 & 0 & 0 \\ 0 & 0 & 1 & 0 \\ 0 & 0 & 0 & e^{i\phi} \end{pmatrix}. \tag{S7}$$

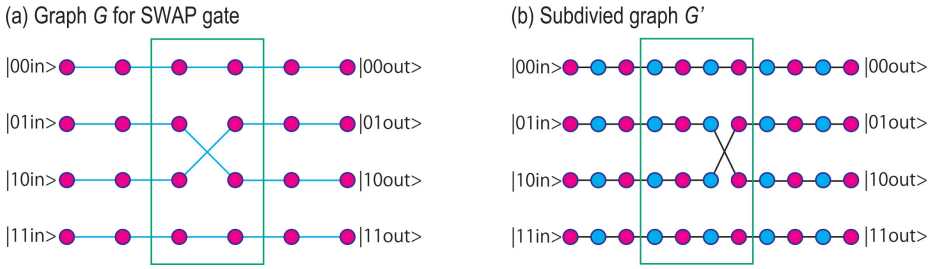


FIG. S1: Graph representation of the SWAP gate, where the $|01\rangle$ and $|10\rangle$ are interchanged.

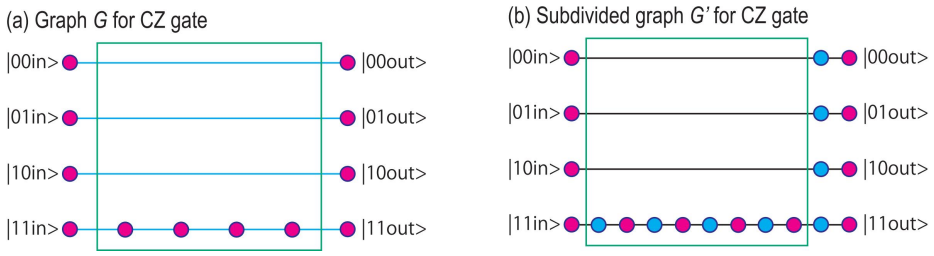


FIG. S2: Graph representation on the CZ gate. It consists of the operation of the π phase-shift gate only for $|11\rangle$.

We realize it by inserting some inductors only to the wire representing $|11\rangle_{\text{out}}$.

Toffoli gate: The Toffoli gate is a controlled-controlled NOT gate defined by

$$U_{\text{Toffoli}} \equiv \begin{pmatrix} I_4 & O_4 \\ O_4 & U_{\text{CNOT}} \end{pmatrix} = \begin{pmatrix} 1 & 0 & 0 & 0 & 0 & 0 & 0 & 0 \\ 0 & 1 & 0 & 0 & 0 & 0 & 0 & 0 \\ 0 & 0 & 1 & 0 & 0 & 0 & 0 & 0 \\ 0 & 0 & 0 & 1 & 0 & 0 & 0 & 0 \\ 0 & 0 & 0 & 0 & 1 & 0 & 0 & 0 \\ 0 & 0 & 0 & 0 & 0 & 1 & 0 & 0 \\ 0 & 0 & 0 & 0 & 0 & 0 & 0 & 1 \\ 0 & 0 & 0 & 0 & 0 & 0 & 1 & 0 \end{pmatrix}, \tag{S8}$$

where I_4 is the four-dimensional identity matrix and O_4 is the four-dimensional null matrix with the three-qubit basis $\{|000\rangle, |001\rangle, |010\rangle, |011\rangle, |100\rangle, |101\rangle, |110\rangle, |111\rangle\}^t$.

$$\begin{pmatrix} |000\rangle_{\text{out}} \\ |001\rangle_{\text{out}} \\ |010\rangle_{\text{out}} \\ |011\rangle_{\text{out}} \\ |100\rangle_{\text{out}} \\ |101\rangle_{\text{out}} \\ |110\rangle_{\text{out}} \\ |111\rangle_{\text{out}} \end{pmatrix} = U_{\text{Toffoli}} \begin{pmatrix} |000\rangle_{\text{in}} \\ |001\rangle_{\text{in}} \\ |010\rangle_{\text{in}} \\ |011\rangle_{\text{in}} \\ |100\rangle_{\text{in}} \\ |101\rangle_{\text{in}} \\ |110\rangle_{\text{in}} \\ |111\rangle_{\text{in}} \end{pmatrix}. \tag{S9}$$

We use eight wires for three-qubit circuits. The two wires $|110\rangle_{\text{in}}$ and $|111\rangle_{\text{in}}$ are interchanged within the widget, while the others are directly connected to the outputs as shown in Fig.S3(a).

Fredkin gate: The Fredkin gate is a controlled SWAP gate defined by

$$U_{\text{Fredkin}} \equiv \begin{pmatrix} I_4 & O_4 \\ O_4 & U_{\text{SWAP}} \end{pmatrix} = \begin{pmatrix} 1 & 0 & 0 & 0 & 0 & 0 & 0 & 0 \\ 0 & 1 & 0 & 0 & 0 & 0 & 0 & 0 \\ 0 & 0 & 1 & 0 & 0 & 0 & 0 & 0 \\ 0 & 0 & 0 & 1 & 0 & 0 & 0 & 0 \\ 0 & 0 & 0 & 0 & 1 & 0 & 0 & 0 \\ 0 & 0 & 0 & 0 & 0 & 0 & 1 & 0 \\ 0 & 0 & 0 & 0 & 0 & 1 & 0 & 0 \\ 0 & 0 & 0 & 0 & 0 & 0 & 0 & 1 \end{pmatrix}. \tag{S10}$$

Similarly to the Toffoli gate, the two wires $|101\rangle_{\text{in}}$ and $|110\rangle_{\text{in}}$ are interchanged within the widget, while the others are directly connected to the outputs as shown in Fig.S3(b).

The $\pi/4$ phase shift gate: In the case of $N = 2$, the momentum is $k_0 = 11\pi/8$. By inserting m inductors in one wire, we may generate the phase shift $2mk_0$ as follows.

m	1	2	3	4	5	6	7	8
phase shift	$\frac{3\pi}{4}$	$\frac{3\pi}{2}$	$\frac{\pi}{4}$	π	$\frac{7\pi}{4}$	$\frac{\pi}{2}$	$\frac{5\pi}{4}$	0

(S11)

We have chosen $m = 3$ in order to realize the $\pi/4$ phase-shift gate in the main text.

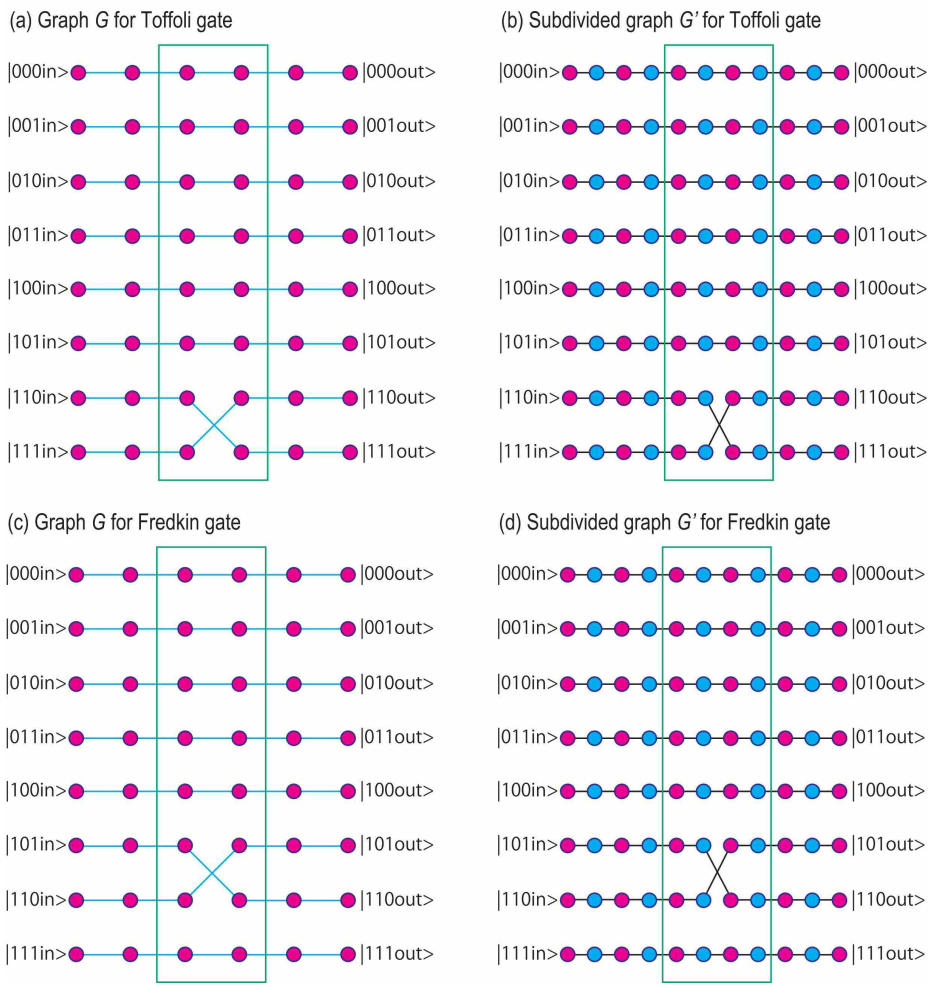


FIG. S3: Graph representations of the (a) Toffoli and (b) Fredkin gates.

The $\pi/8$ phase shift gate: In the case of $N = 4$, the momentum is $k_0 = 21\pi/16$. By inserting m inductors in one wire, we may generate the phase shift $2mk_0$ as follows.

m	1	2	3	4	5	6	7	8	9	10	11	12	13	14	15	16
phase shift	$\frac{5\pi}{8}$	$\frac{5\pi}{4}$	$\frac{15\pi}{8}$	$\frac{\pi}{2}$	$\frac{9\pi}{8}$	$\frac{7\pi}{4}$	$\frac{3\pi}{8}$	π	$\frac{13\pi}{8}$	$\frac{\pi}{4}$	$\frac{7\pi}{8}$	$\frac{3\pi}{2}$	$\frac{\pi}{8}$	$\frac{3\pi}{4}$	$\frac{11\pi}{8}$	0

(S12)

We choose $m = 13$ in order to realize the $\pi/8$ phase shift gate.

QFT with $N = 4$: The QFT for $N = 4$ is explicitly given by

$$U_{\mathrm{QFT2}} = \frac{1}{2}\begin{pmatrix} 1 & 1 & 1 & 1 \\ 1 & i & -1 & -i \\ 1 & -1 & 1 & -1 \\ 1 & -i & -1 & i \end{pmatrix}. \tag{S13}$$

It is decomposed into the sequential applications of the SWAP gate, the Hadamard gate and the controlled-phase-shift gate $U_{2\to\phi}$ as

$$U_{\mathrm{QFT2}} = (U_{\mathrm{H}} \otimes I_2)\left(U_{2\to\pi/2}\right)(I_2 \otimes U_{\mathrm{H}})\, U_{\mathrm{SWAP}}, \tag{S14}$$

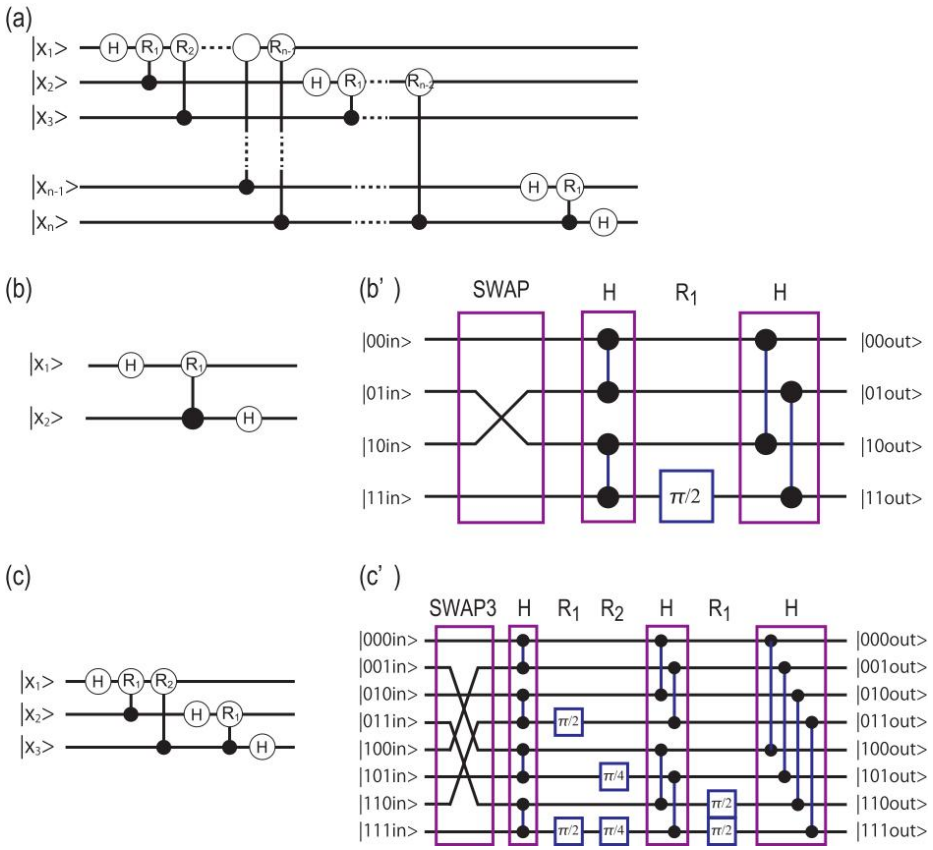


FIG. S4: (a) Quantum circuit representation of quantum Fourier transformation. The symbol R_n indicates the $\pi/2^n$ phase-shift gate and H indicates the Hadamard gate. (b) Two-qubit quantum Fourier transformation. (c) Three-qubit quantum Fourier transformation. (b'), (c') The corresponding reduced graph representation.

where

$$I_2 \otimes U_{\rm H} = \frac{1}{\sqrt{2}} \begin{pmatrix} 1 & 1 & 0 & 0 \\ 1 & -1 & 0 & 0 \\ 0 & 0 & 1 & 1 \\ 0 & 0 & 1 & -1 \end{pmatrix}, \quad U_{\rm H} \otimes I_2 = \frac{1}{\sqrt{2}} \begin{pmatrix} 1 & 0 & 1 & 0 \\ 0 & 1 & 0 & 1 \\ 1 & 0 & -1 & 0 \\ 0 & 1 & 0 & -1 \end{pmatrix}, \quad U_{2\to\pi/2} = \begin{pmatrix} 1 & 0 & 0 & 0 \\ 0 & 1 & 0 & 0 \\ 0 & 0 & 1 & 0 \\ 0 & 0 & 0 & i \end{pmatrix}. \tag{S15}$$

QFT with $N = 8$: The QFT for $N = 8$ is explicitly given by

$$U_{\rm QFT3} = \frac{1}{2\sqrt{2}} \begin{pmatrix} 1 & 1 & 1 & 1 & 1 & 1 & 1 & 1 \\ 1 & \omega & \omega^2 & \omega^3 & \omega^4 & \omega^5 & \omega^6 & \omega^7 \\ 1 & \omega^2 & \omega^4 & \omega^6 & 1 & \omega^2 & \omega^4 & \omega^6 \\ 1 & \omega^3 & \omega^6 & \omega & \omega^4 & \omega^7 & \omega^2 & \omega^5 \\ 1 & \omega^4 & 1 & \omega^4 & 1 & \omega^4 & 1 & \omega^4 \\ 1 & \omega^5 & \omega^2 & \omega^7 & \omega^4 & \omega & \omega^6 & \omega^3 \\ 1 & \omega^6 & \omega^4 & \omega^2 & 1 & \omega^6 & \omega^4 & \omega^2 \\ 1 & \omega^7 & \omega^6 & \omega^5 & \omega^4 & \omega^3 & \omega^2 & \omega \end{pmatrix} \tag{S16}$$

with $\omega = e^{i\pi/4}$.

It is decomposed into the sequential applications of the three-qubit SWAP gate $U_{\rm SWAP3}$, the Hadamard gate and the controlled-phase-shift gate $U_{n\to\phi}$ as

$$U_{\rm QFT3} = (U_{\rm H} \otimes I_2 \otimes I_2)\left(U_{3\to\pi/2}\right)(I_2 \otimes U_{\rm H} \otimes I_2)\left(U_{3\to\pi/4}\right)\left(U_{2\to\pi/2}\right)(I_2 \otimes I_2 \otimes U_{\rm H})\, U_{\rm SWAP3}, \tag{S17}$$

with

$$U_{2\to\pi/2} = \text{diag.}\,[1,1,1,i,1,1,1,i] \tag{S18}$$

$$U_{3\to\pi/4} = \text{diag.}\left[1,1,1,1,1,e^{i\pi/4},1,e^{i\pi/4}\right] \tag{S19}$$

$$U_{3\to\pi/2} = \text{diag.}\,[1,1,1,1,1,1,i,i] \tag{S20}$$

and

$$U_{\text{SWAP3}}\,|j_3 j_2 j_1\rangle = |j_1 j_2 j_3\rangle \tag{S21}$$

with

$$U_{\text{SWAP3}} = \begin{pmatrix} 1 & 0 & 0 & 0 & 0 & 0 & 0 & 0 \\ 0 & 0 & 0 & 0 & 1 & 0 & 0 & 0 \\ 0 & 0 & 1 & 0 & 0 & 0 & 0 & 0 \\ 0 & 0 & 0 & 0 & 0 & 0 & 1 & 0 \\ 0 & 1 & 0 & 0 & 0 & 0 & 0 & 0 \\ 0 & 0 & 0 & 0 & 0 & 1 & 0 & 0 \\ 0 & 0 & 0 & 1 & 0 & 0 & 0 & 0 \\ 0 & 0 & 0 & 0 & 0 & 0 & 0 & 1 \end{pmatrix}. \tag{S22}$$